



# The dynamics of a young protostellar core

E. Redaelli, F. O. Alves, P. Caselli, J. E. Pineda, and the GAS team

Max Planck Institut für Extraterrestrische Physik, Giessenbachstrasse 1, D-85748, Garching, Germany, e-mail: eredaelli@mpe.mpg.de

**Abstract.** The first stages of star formation represent a research field of ongoing development from the theoretical point of view, and molecular line observations are needed to shed light on the dynamical evolution of star-forming regions and constrain theories. We have investigated the Barnard 59 core (hereafter B59), the very western end of the Pipe Nebula. This elongated and filamentary molecular cloud, located at a distance of 145 pc (Alves & Franco 2007), is known to have a low star formation efficiency (0.06%, Forbrich et al. 2009). The only active site of star formation is B59, with  $\sim 20$  young stellar objects (YSOs) identified by the Spitzer Cores to Disks survey (Brooke et al. 2007). Using ammonia inversion transition lines (1,1) and (2,2), we achieved a comprehensive view of the kinematic properties of the source, investigating at the same time the role of protostellar feedback. Additional dust thermal emission was used to obtain dust temperature and  $H_2$  column density maps. More details on the present work will be given in Redaelli et al (subm.).

## 1. Observations and data analysis

The ammonia (1,1) and (2,2) spectral data were acquired at the Green Bank Telescope (GBT) as part of the Green Bank Ammonia Survey (GAS) Large Program (Friesen et al. 2017). The achieved spectral resolution is  $\approx 0.07 \text{ km s}^{-1}$  and the angular resolution is  $31.8''$ , corresponding to  $0.02 \text{ pc}$  at the Pipe distance. The data were smoothed to a final resolution of  $40''$  to improve the signal-to-noise ratio.

The spectral cubes were fitted pixel by pixel in order to obtain the following parameter maps: excitation temperature  $T_{ex}$ , kinetic temperature  $T_K$ , centroid velocity  $V_{lsr}$ , velocity dispersion  $\sigma_V$ , and ammonia column density  $N(\text{NH}_3)$ . Furthermore, we used Herschel SPIRE data at  $250 \mu\text{m}$ ,  $350 \mu\text{m}$  and  $500 \mu\text{m}$  to characterize the dust emission. These three photometric bands were fitted with a grey-body model to recover the  $H_2$  column density and the dust temperature  $T_{dust}$  maps.

## 2. Kinematic structure

The source presents a cold ( $T_K \approx 11 \text{ K}$ ) region where  $\log[N(\text{NH}_3)]$  is large ( $> 14.4 \text{ cm}^{-2}$ ), the centroid velocity shows a coherent structure and the velocity dispersion exhibits values as low as  $0.11 - 0.13 \text{ km s}^{-1}$  (see Fig. 1). Towards North, the temperature increases up to  $16 - 18 \text{ K}$ , possibly indicating that another source of heating, in addition to the cosmic ray field or radiation field, is needed. This can be due to the activity of BHB07-11 (B11), the youngest YSO in the cluster (Class 0/I, circle marker in the figures) that is powering a bipolar outflow (Duarte-Cabral et al. 2012). The linewidths increment in this area can also be due to the protostellar activity.

## 3. Turbulence in the core

Using the  $\sigma_V$  and  $T_K$  maps we calculated the thermal  $\sigma_T$  and non thermal  $\sigma_{NT}$  velocity dispersion contribution and the sonic

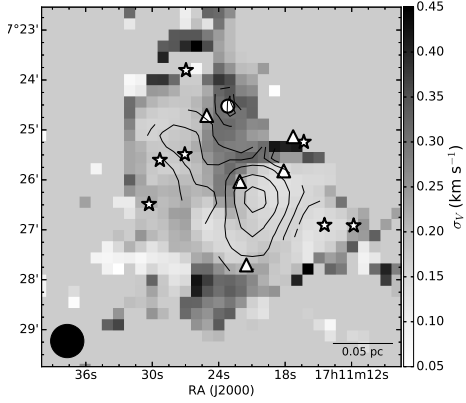


**Fig. 1.**  $\sigma_V$  map with  $\log[N(\text{NH}_3)]$  contours (levels: 14.0, 14.2, 14.4, 14.6, 14.75). Markers show the YSOs positions (circle: class 0/I, triangles: class I or II, stars: class II) according to Brooke et al. (2007).

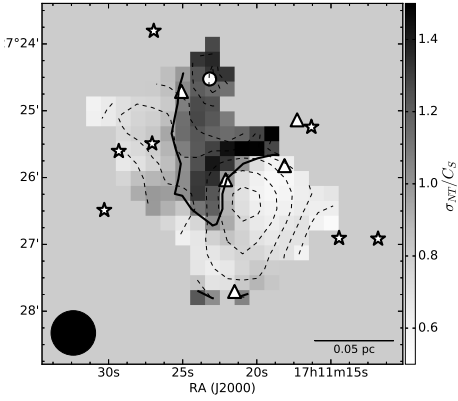


**Fig. 2.**  $\sigma_{NT}/C_S$  map. The dashed contours and markers are the same as in Fig. 1. The black curve represents where  $\sigma_{NT}/C_S = 1$ .

speed  $C_S$ , obtaining the  $\sigma_{NT}/C_S$  map shown in Fig. 2. The coldest and densest part of the core presents subsonic motions, with a sharp transition to mildly supersonic ones in the northern region. This enhancement in the turbulence level can be linked to the B11 activity, which is affecting the surrounding medium. Most of the other YSOs, and especially the most evolved class II ones, are located in subsonic, low velocity dispersion regions and most likely are foreground or background objects, not embedded anymore in the cloud.

### 3.1. $\text{H}_2$ and $\text{NH}_3$ comparison

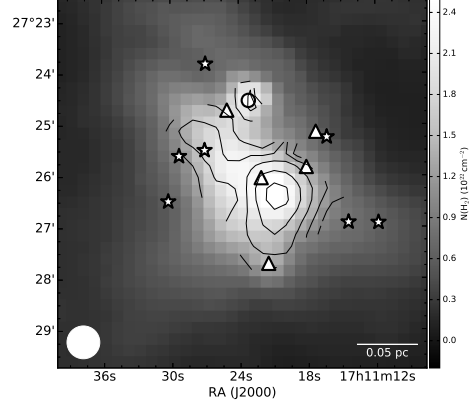


**Fig. 3.**  $N(\text{H}_2)$  map with  $\log[N(\text{NH}_3)]$  contours. The levels and the markers code are the same as before.

Fig. 3 shows the  $N(\text{H}_2)$  map obtained from Herschel data with the contours from  $N(\text{NH}_3)$ . As expected, ammonia is a good tracer of the cold gas (Ho & Townes, 1983), with the exception of the B11 envelope, which is very bright in Herschel data but seems to be depleted in ammonia. This can be due to chemical effects: at  $T \approx 20 \text{ K}$  (close to the values we found) CO starts to evaporate from dust grain and it can inhibit the formation of  $\text{NH}_3$  precursors (Rodgers & Charnley 2008).

### References

- Alves, F. O. & Franco, G. A. P. 2007, *A&A*, 470, 597
- Brooke, T. Y., et al. 2007, *ApJ*, 655, 364
- Duarte-Cabral, A., et al. 2012, *A&A*, 543, A140
- Forbrich, J., et al. 2009, *ApJ*, 704, 292
- Friesen, R. K., et al. 2017, *ApJ*, 843, 63
- Ho, P. T. P. & Townes, C. H. 1983, *ARA&A*, 21, 239
- Rodgers, S. D. & Charnley, S. B. 2008, *ApJ*, 689, 1448